Paleoceanography and Paleoclimatology

RESEARCH ARTICLE
10.1029/2020PA004144

Assessing Sedimentary Detrital Pb Isotopes as a Dust Tracer in the Pacific Ocean

Andrea M. Erhardt[1], Grant Douglas[2], Andrew D. Jacobson[3], Josh Wimpenny[4], Qing-Zhu Yin[4], and Adina Paytan[5]

[1]Department of Earth and Environmental Sciences, University of Kentucky, Lexington, KY, USA, [2]CSIRO Land and Water, Wembley, WA, Australia, [3]Department of Earth and Planetary Sciences, Technological Institute, Northwestern University, Evanston, IL, USA, [4]Department of Earth and Planetary Sciences, University of California, Davis, Davis, CA, USA, [5]Institute of Marine Sciences, University of California Santa Cruz, Santa Cruz, CA, USA

Key Points:

- Pb isotopic ratios of detrital fractions provide general trends but not definitive determination of dust source regions
- Mixing models are sensitive to small changes in source isotopic values, highlighting importance of accurate source characterization
- Glacial/Interglacial downcore variability in Pb isotopic ratios reflect climate-driven dust delivery to the Eastern Equatorial Pacific

Supporting Information:

Supporting Information may be found in the online version of this article.

Correspondence to:

A. M. Erhardt,
andrea.erhardt@uky.edu

Citation:

Erhardt, A. M., Douglas, G., Jacobson, A. D., Wimpenny, J., Yin, Q.-Z., & Paytan, A. (2021). Assessing sedimentary detrital Pb isotopes as a dust tracer in the Pacific Ocean. *Paleoceanography and Paleoclimatology*, *36*, e2020PA004144. https://doi.org/10.1029/2020PA004144

Received 6 OCT 2020
Accepted 4 MAR 2021

Abstract Mineral dust particles from different source regions typically have distinct Pb isotope ratios. Theoretically, Pb isotopic composition of terrigenous minerals isolated from open-ocean sediments should allow for dust provenance reconstructions. However, Pb isotopes of terrigenous fractions of sediments have frequently been inconsistent with expected source region signatures. This study investigates the reason(s) for offsets between the Pb isotope values of the dust component in sediment cores and those expected from source regions with focus on changes in sediment composition, sediment age, and sediment processing for analysis. Pb isotope ratios from Pacific Ocean core-top sediments show a general delineation of the Intertropical Convergence Zone (ITCZ). Isotope mixing models support these general trends, though similarity in Pb isotope ratios of disparate source regions makes constraining specific sources challenging. Pb isotope ratios in downcore samples varied on glacial/interglacial time scales, being less radiogenic during the last glacial maximum, suggesting either a weakened ITCZ or the addition of a new, less radiogenic, source to the system. Finally, Pb isotope ratios in some source region samples yielded different Pb isotope signatures in bulk source sample than in the insoluble terrigenous fraction of the source sample, indicating that differential mineral preservation within the terrigenous component in sediments may cause offsets from source signatures. Overall, while Pb isotopes show distinct basin-scale variations, high-resolution spatial reconstructions require tight age controls and consistency in analytical treatment if used to define ocean sediment source regions.

Plain Language Summary Dust deposited in the open ocean is sourced from rocks and sediment of various ages and location. The trace amounts of lead in this dust can have distinct isotopic values, theoretically allowing for reconstruction of dust sources. This paper looks at lead isotopes in dust deposited in the Pacific Ocean, specifically the Eastern Equatorial Pacific. Our objective is to understand how well this reconstruction tool works and if it can tell us how dust deposition has changed over glacial cycles. We found that lead isotopes work well to generally distinguish between Northern and Southern Hemisphere dust, though poor characterization and isotopic composition variability within smaller regions makes definitive source determination difficult. However, we did see changes over glacial climate cycles in the Eastern Equatorial Pacific, resulting from either change in wind patterns and/or the addition of a new dust source. Finally, we highlight the importance of consistent sample preparation to limit additional variability. Overall, lead isotopes can distinguish between some source trends, though work best when combined with other dust source tracers.

1. Introduction

Determining source regions and fluxes of aeolian dust deposition to the open ocean can provide insight into atmospheric circulation patterns, climate, and aridity, and may have implications for ocean productivity and carbon sequestration (Martin, 1990; Paytan et al., 2009; Winckler et al., 2008; Xie & Marcantonio, 2012). The source and quantity of dust reaching a particular site can vary with climate and anthropogenic changes to landscapes and with changes in the strength and trajectory of winds (Rea, 1994), with advective transport with in the water column at most a second-order effect (Anderson et al., 2016). In particular, dust loads can be impacted by changes in climatic conditions, which affect wind dynamics and alter the aridity of the source regions and their land cover (Maher et al., 2010). Moreover, different sources of dust have

been shown to induce diverse responses in ocean primary productivity and plankton community structure (Chien et al., 2016; Mackey et al, 2010, 2012). Therefore, it is important to identify how dust deposition sources have changed spatially and temporally.

Pb isotopes have been used in a range of studies to trace aeolian dust flux sources (Jones et al., 2000; Pettke et al., 2000; Pichat et al., 2014; Stancin et al., 2006) and to reconstruct changes in the location of the ITCZ (Reimi et al., 2019; Reimi & Marcantonio, 2016; Xie & Marcantonio, 2012). The premise is that since different dust source regions are of different ages and have different lithologies, and therefore distinct stable Pb isotope ratios, it should be possible to discern the relative contribution of these different sources using source apportion mixing models. Indeed, this approach has worked well with other isotope systems. For example, Nd isotopes in sediment detrital fractions generally show clear latitudinal delineation, with progressively more northern sourced dust in northern locations (Bayon et al., 2020; Reimi et al., 2019; Xie & Marcantonio, 2012).

Pb isotopes in sediment detrital fractions also show ocean-scale trends, with distinct differences between Northern and Southern Hemisphere samples (Jones et al., 2000; Pichat et al., 2014; Stancin et al., 2006). However, when regional Pb records are considered, particularly north-south transects that span the ITCZ, the Pb isotope records alone do not show the expected separation of Northern and Southern Hemisphere dust sources (Xie & Marcantonio, 2012). Several suggestions have been put forth to explain why Pb isotopes do not show clear regional signatures of dust provenance when used alone. Specifically, it is possible that the source material itself is highly heterogeneous and/or that different dust constituents are differentially preserved in the sedimentary record (Arimoto, 2001). It is also possible that the methods used for sample preparation result in preferential dissolution of different phases (Hyeong et al., 2011). Anthropogenic contamination of the samples used to characterize the source may also be a factor (Grousset & Biscaye, 2005).

Multiple studies have been undertaken to constrain source region variability in Pb isotopes (Höfig et al., 2016; Pettke et al., 2000; Pichat et al., 2014; Stancin et al., 2006, and references therein). For example, in Höfig et al. (2016), 2,014 samples from the GEOROC database were compiled to capture the range and variability in source area signatures. While Höfig et al. (2016) provide isotopic bounds for each source region, there are some shortcomings. First, most of the samples used are from igneous rocks, and while weathering of igneous rocks is an important dust sources, these results are biased against sedimentary rocks that may be more readily weathered. Moreover, using rocks rather than soil or dust samples does not account for incongruent weathering. Additionally, dust may also inherit Pb from other sources during the weathering cycle and transport to the ocean. Finally, different sequential leaching procedures have been employed for delineating terrigenous sources in ocean sediments, which could bias source reconstructions.

Given the low concentration of Pb in many marine sediments, the addition of anthropogenic Pb to the sediment from authigenic phases remains a concern. While anthropogenic Pb has a range of isotopic values, typically the values are less radiogenic than natural dust sources (Gallon et al., 2011; Zurbrick et al., 2017) and possess distinctive isotopic signatures. Therefore, even a small amount of anthropogenic contamination can impact the Pb isotopic signature of a sample. However, while contamination cannot be always eliminated, the unique signature of anthropogenic Pb and the ability to use multiple isotope ratios in the Pb system can help identify contaminated samples and remove them when studies are interested in natural preanthropogenic processes.

In this study, we consider some of the potential influences on the Pb isotopic signature of the detrital fraction in open-ocean sediments that may confound identifying source signatures. While redefining the established Pb isotope compositions of source regions is outside the scope of this project, we consider the impact of sample treatment such as leaching procedures on the robustness of source region characterizations. We analyze the Pb isotopes of the operationally defined terrigenous fraction of sediments from the upper 10 cm of piston cores across the Pacific to help illustrate regional (adjacent cores) and site specific (within one core) variability. The impact of anthropogenic contamination is also considered. Finally, we present a downcore record for core TTN013-PC72 at the equator at 140°W, compare this record to previously published data from equatorial Pacific cores and discuss the impact of imprecise age models on the record.

2. Methods

2.1. Sample Materials

Loess, silt, and basalt samples from several potential dust source regions with different published bulk Pb isotope signatures (Stancin et al., 2006; Vallelonga et al., 2010) were obtained and processed using the sequential leaching method described below. These samples include Chinese loess, New Zealand loess, Australian loess, Galapagos Island basalts, and South American (Atacama Desert) and North American silt. We focus on loess and silt samples, as these are more representative of potential dust transported to the open ocean than the bulk rocks. The locations of these samples are listed in Table S1. These locations and samples were selected to best represent potential eolian material and, when possible, to capture regional variability where it is likely to exist, such as in China and the Atacama Desert. Samples were excavated from the subsurface to minimize impacts of anthropogenic Pb contamination. Samples were freeze dried at the University of California Santa Cruz (UCSC) and then dry sieved through plastic mesh to isolate the <63 μm fraction, representative of wind-blown sediment (Ridame & Guieu, 2002).

The Chinese loess samples are from a Chinese loess plateau transect, along 108°E between 34°N and 37°N. Detailed sample locations and collection information can be found in Yang and Ding (2003). Additional geochemical information for the Chinese loess samples, including percent calcium carbonate and strontium isotope ratios, can be found in Jacobson (2004).

New Zealand loess was collected from the beach cliffs outside the town of Oamaru at 45.084°S, 170.988°E. Loess at this location is thought to have been deposited during the Last Glacial Maximum (Worthy & Grant-Mackie, 2003) and represents material that could have been transported to the Pacific. Australian dust was characterized using samples from the B soil horizons in the Bago-Maragle forest and a site near the town of Brucedale in New South Wales, Australia, obtained from the CSIRO National Soil Collection.

Samples from the Atacama Desert were obtained from five transects spanning 20°S to 36°S collected from multiple alluvial fan settings at a depth of 25–30 cm below the surface. To characterize the impact that volcanic material, particularly volcanic ash that may have arrived at the eastern equatorial Pacific (EEP), fresh basalt from the Galapagos Islands was obtained and prepared as discussed in section 2.2.

Samples from the Channel Islands off the coast of southern California were collected differently from samples in the other regions, namely they represent soil samples that required additional separation steps to isolate the silt fraction (Muhs et al., 2007). However, they are included as representatives of combined North American source regions. The silt deposited on these islands has been transported from North America and gives an integrated representation of dust that is transported to mid-latitude North Pacific coastal regions (Muhs et al., 2007). Samples were obtained from three islands defining a ~160 km north-south transect, East Anacapa Island, Santa Barbara Island, and San Clemente Island. Further description of the samples and collection methods can be found in Muhs et al. (2007, 2008).

To construct a survey of Pb isotopes in the detrital fraction of core-top sediments, samples from across the Equatorial Pacific, with a focus on the EEP, were obtained from the Oregon State and Scripps Institution of Oceanography core repositories. Cores were selected to provide tight spatial coverage within the EEP, with multiple north-south transects and with samples along the equator from 90°W to 140°W. The location and water depth of the samples are given in Table S2. All samples were from the upper 10 cm of the core, and typically the upper 5 cm. In addition, a handful of samples from across the greater Pacific Ocean were processed to provide context to the detailed EEP investigation. Locations and water depths of these samples are listed in Table S3. It should be noted that while attempts were made to verify the ages of the core-top samples to ensure they were Holocene, that information was not always available for all sites and dating each sample was outside the scope of this work.

To reconstruct changes in the dust sources to the equatorial Pacific region over time, downcore samples from TTN013-PC72 (0.1°N, 139.4°W, Figure 1) were obtained at roughly 10 cm depth resolution for the upper 200 cm of the core, representing a record of ~100 ka. Detailed core description and the age model for this core are given in Murray et al. (2000).

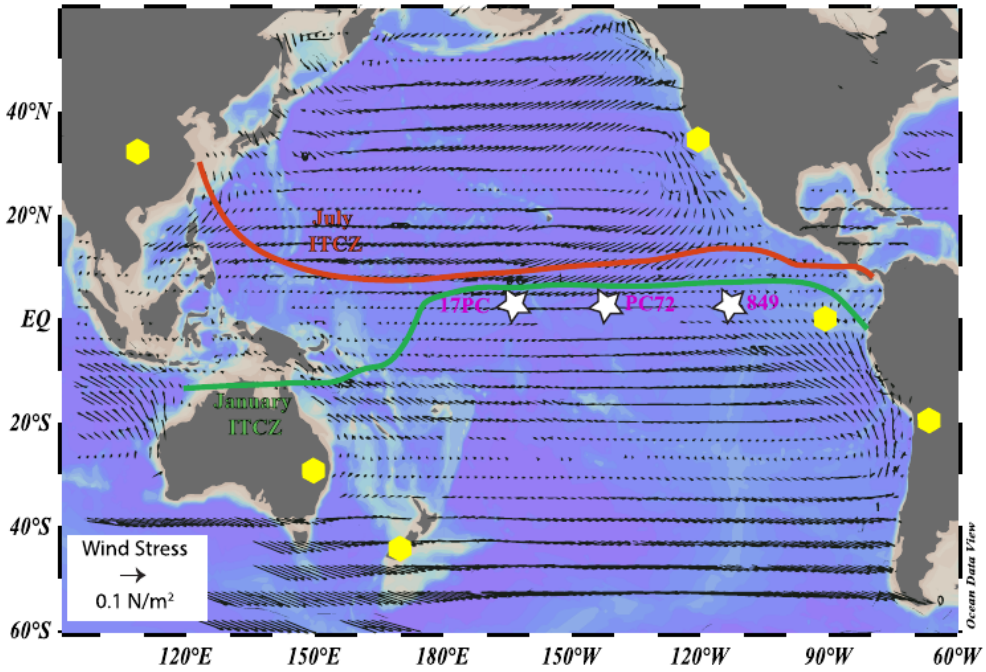

Figure 1. Overview map of modern wind patterns and ITCZ location for the Pacific Ocean. Winter wind vector map is from Kalnay et al. (1996) and ITCZ locations are from Liu et al. (2015). Site 17PC represents downcore studies from Reimi et al. (2016, 2019), Site 849 includes work by Pichat et al. (2014) and Xie and Marcantonio (2012), and PC72 is presented in this study. Source region sample locations used in this study are shown in yellow. ITCZ, Intertropical Convergence Zone.

2.2. Analytical Methods

No consistently used method currently exists to isolate a pure terrigenous dust fraction from sediments. Nevertheless, one can optimize comparisons between source and sediment samples by processing them identically. As such, an operationally defined detrital fraction, consisting predominantly of silicates, was isolated from each sample (source samples and sediments) using a sequential leaching procedure as described below. This fraction represents the silicate fraction of the eolian component in sediments; however, it may also include noneolian insoluble material, such as marine barite or rutile from submarine volcanic activity. In contrast, some eolian components such as terrigenous carbonate minerals are lost in the process.

Most samples were freeze dried at the University of California Santa Cruz (UCSC) and then dry sieved through plastic mesh to isolate the <63 μm fraction, representative of wind-blown sediment (Ridame & Guieu, 2002). As the Galapagos Basalt sample was a fresh hand sample, it was prepared to simulate dust and allow for similar chemical leaching conditions as other samples. After removing the outer portion of a basalt hand sample to avoid anthropogenic Pb, the inner portion was crushed using a ceramic mortar and pestle and sieved to <63 μm. The North American samples were processed differently because these were soil samples and the detrital fraction had to be separated from soils. For these samples, the silt size fraction (2–53 μm) was isolated from the soil, organic matter was removed with hydrogen peroxide, and sodium hexametaphosphate, in combination with ultrasonic shaking, was used as a dispersant. The clays were then removed by utilizing Stokes Law through repeated sedimentation and siphoning, isolating the 2–53 μm fraction.

Approximately 150 mg of each sample were weighed and placed in acid-cleaned 50 mL centrifuge tubes. Primary or secondary carbonate and ferromanganese precipitates were removed from the sediment following methods modified from Gutjahr et al. (2007). Specifically, carbonates were removed using a mixed sodium acetate/acetic acid solution; the lightly bound Pb was removed via $MgCl_2$ solution-induced cation exchange, and two repeats of a buffered NH_2OH/EDTA solution treatment were added sequentially and allowed to react overnight to ensure all oxyhydroxides were removed. Samples were rinsed with ultrapure

water three times between each step. The residual sediment was treated with H_2O_2 to remove organic material, rinsed 3 times with ultrapure water, and transferred to acid-cleaned Teflon vials. These samples were digested over 72 h on a 90°C hotplate in three sequential steps: 50:50 mixture of 14N quartz distilled HNO_3 and 22.6N Optima grade HF, dried, and redissolved overnight in 6N quartz distilled HCl; and dried and redissolved overnight in 7N quartz distilled HNO_3. Bulk sediment samples (e.g., without the pretreatment) were also digested in Teflon vials as described above for comparison. Reagent and method blanks were monitored throughout the process. Typically, the blank contribution was less than 1% of the sample.

To prepare all samples for Pb isotope analysis, each digested sample was dried and redissolved in 100 μL of concentrated Optima grade HBr. This fraction was gently dried, and the process repeated to ensure the predominance of an HBr matrix. The sample was then redissolved in 1N HBr for column separation. Chemical separation was achieved using 10 cm Teflon columns packed with AG1-X8 anion resin (adapted from Kamber & Gladu, 2009). Approximately 600 μL of resin was cleaned with quartz distilled 6N HCl and conditioned with 1N HBr. The sample was then loaded onto the columns and washed with 2.2 mL of 1N HBr followed by 1 mL 2N distilled HCl. To elute the retained Pb, 2.2 mL of 6N distilled HCl was added and collected in a separate acid-cleaned Teflon vial. The sample was dried and reconstituted in 0.28N Optima grade HNO_3 for isotope and Pb concentration analyses. All work was conducted in a Class 1000 clean lab facility at the University of California at Santa Cruz (UCSC).

2.3. Pb Concentration and Isotope Ratio Measurements

Concentrations of Pb were determined using an Element ICP-MS at UCSC on an aliquot of the samples and a subset of samples was also analyzed for other elements (Al, Fe, Zr, Ba, U). The 0.28N HNO_3 used for reconstitution contained 1 ppb of both Bi and Rh to allow correction of instrument drift. A calibration curve was constructed at the start of the analytical run using a serial dilution of ICP-MS element standards, with standards monitored every 6–12 samples. Overall, the standard deviation of a 1 ppb Pb standard was 0.012 ppb over the duration of a run after any drift correction. The internal sample standard deviation ranged from 0.06% to 2% (average ~1%) depending on the size of the sample measured. Additionally, three aliquots of a subset of samples were run every 10–20 samples, with a reproducibility of ~5%.

Pb isotope ratios ($^{206}Pb/^{204}Pb$, $^{207}Pb/^{204}Pb$, and $^{208}Pb/^{204}Pb$) were measured using a Neptune MC-ICP-MS either at the University of California Santa Cruz (UCSC) or Davis (UCD). Samples were introduced into the instrument using a CETAC MCN 6000 desolvating nebulizer at UCSC and an APEX desolvating nebulizer at UCD, in combination with a high efficiency X-cone. The former configuration has been shown to maximize both precision and accuracy for sample concentrations <10 ppb (Gallon et al., 2008) on the UCSC Neptune MC-ICP-MS. Sensitivity averaged 5–10 V on ^{208}Pb for a 15 ppb standard solution, and samples were diluted as necessary to keep sample sizes between 5 and 20 V on ^{208}Pb. Sample concentrations above 3 ppb, resulting in at least 1 V of ^{208}Pb, had internal 1σ run standard deviations of <0.003 for $^{206}Pb/^{204}Pb$. Both Ar and N_2 flows were optimized for maximum sensitivity during each run. Between samples, a 2% HNO_3 solution was introduced until the monitored ^{208}Pb signal dropped below 0.002 V. Data collection was preformed over 50, 1-s cycles, with a 90 s uptake time. A 2σ rejection of outliers was preformed automatically.

After allowing the plasma to stabilize for 1.5 h and tuning the instrument to optimize sensitivity, NIST SRM 981 was repeatedly analyzed to ensure accuracy and reproducibility. After establishing the stability and reproducibility of Pb ratios for SRM 981, samples were introduced, and SRM 981 was reanalyzed every five samples. Inter-run 2σ standard deviation (2σSD) of all samples averaged 0.002 for $^{206}Pb/^{204}Pb$, 0.022 for $^{207}Pb/^{204}Pb$, and 0.065 for $^{208}Pb/^{204}Pb$. Over the lifetime of this project and concurrent projects measuring Pb isotopes, 256 analyses of Pb SRM 981 were conducted. These analyses resulted in $^{206}Pb/^{204}Pb$ of 16.932 (2σSD 0.006), $^{207}Pb/^{204}Pb$ of 15.482 (2σSD 0.005), and $^{208}Pb/^{204}Pb$ of 36.671 (2σSD 0.02). Because the measured standard ratios were consistently slightly less than the certified ratios for NIST SRM 981 (Galer, 1999), sample ratios were normalized to the certified ratio using sample/standard bracketing.

Instrumental mass bias was corrected using the exponential law through Tl addition. Since the mass range of Tl overlaps that of Pb, the addition of a Tl standard with a known isotopic composition (NIST SRM 997) can be used to correct for mass bias (Kamenov et al., 2004). The Tl was added to the samples to achieve a Tl/Pb concentration ratio of 0.2 (Gallon et al., 2008). Data were corrected using a $^{205}Tl/^{203}Tl$ ratio of 2.3871,

based on the certified ratio of SRM 997. To evaluate the similarity of Tl to Pb fractionation between samples and standards, the exponential law mass fractionation factors (β) were monitored throughout the run to ensure that samples and standards had similar values resulting in a consistent correction for instrumental mass fractionation (e.g., White et al., 2000). To evaluate reproducibility, 10% of the samples were processed in triplicate. The 2σSD of these sample sets averages 0.02 $^{206}Pb/^{204}Pb$, 0.005 $^{207}Pb/^{204}Pb$, and 0.023 $^{208}Pb/^{204}Pb$. Finally, a procedural blank, representing the entirety of the sample preparation, was processed every 20 samples. Sample blanks were too low in concentration to achieve a reliable isotopic measurement, with blanks averaging 1–5% of the sample concentration (10–50 pg for a full procedural blank). In addition, the SRM 981 was processed using the same column protocol applied to samples to document precision and verify the lack of Pb isotope fractionation during the sample preparation process.

To quantify the contributions of dust from various sources, the isotope mixing model simmr was used (Parnell, 2020). This R model solves mixing equations for stable isotope data using a Bayesian framework. These simulations were run for both the source areas determined in this study and from literature compilations. Mixing models were run using both the likely published sources and source values from this study to compare the impact of using bulk versus the operationally defined terrigenous fractions of source regions.

Published source area average values and standard deviations were taken from the compilation in Pichat et al. (2014). As this compilation did not have an average Pb isotopic value for North American dust, the value from Stancin et al. (2008) was used. New Zealand loess average value was from this study. Likely source regions were determined based on those identified in previous dust isotopic studies along with some source regions that were specifically close to our sediment sampling sites. Asian dust has been established as a predominant dust source to both hemispheres and has been included as a potential source in all regions. For the North Pacific, source regions used were consistent with Stancin et al. (2006) and Jones et al. (2000). While Asian and North American dust have been proposed as the most likely sources, Galapagos Basalts, Central American dust, and the South American NVZ and SVZ were also included due to proximity to our sediment sampling sites. Indeed, Pichat et al. (2014) identified the SVZ and south CVZ as the dominant end members for samples from ODP849 in the eastern equatorial Pacific. Additionally, Papua New Guinea volcanics were included for equatorial and Southern Hemisphere samples based on the suggestion by Ziegler et al. (2008) of far-reaching transport of this source via the Equatorial Undercurrent. For the Southern Hemisphere samples, dominant sources from Li et al. (2008) were used. They found that Australian and South American Sources as well as Asian dust are the dominant sources.

3. Results

Pb isotopic results for the bulk and residual fractions of the source regions show distinct differences, with some samples having similar bulk and detrital values while others showing differences between these two fractions (Table S1 and Figure 2). Overall, Australian and New Zealand silts are the most radiogenic, Chinese and North American are less radiogenic, and the South American and Galapagos samples are the least radiogenic. Although the North American samples were prepared differently than other source samples in this study and those reported in the literature, results were in general agreement with other studies for North American dust.

To allow for comparison to published data sets, select bulk source samples were analyzed (Table S1). On average, the $^{206}Pb/^{204}Pb$ ratios for the residual (post leaching) fraction were less radiogenic than the bulk fractions by about 0.1, though there was variability in this offset. The differences between the New Zealand bulk and residual fractions were substantially greater, with the $^{206}Pb/^{204}Pb$ of the residual fraction being more radiogenic than bulk sample by 0.5. This difference was less pronounced for the South American samples, with the residual fraction only 0.05 more radiogenic than the bulk sample. As bulk Chinese loess samples were not available, the bulk and silicate fractions from Jones et al. (2000) are used for comparison.

For the core-top detrital samples, $^{207}Pb/^{204}Pb$ ratios vary from 15.59 to 15.68, with most samples, particularly in the EEP, clustering around 15.63–15.64 (Table S2 and Figure 3). The least radiogenic ratios are generally located near coastal settings, particularly near Alaska and Central America. Conversely, the most radiogenic samples are located north of the equator at 140°W, as well as at open-ocean locations in the northwestern Pacific. These trends are also generally observed also in $^{206}Pb/^{204}Pb$ and $^{208}Pb/^{204}Pb$ ratios.

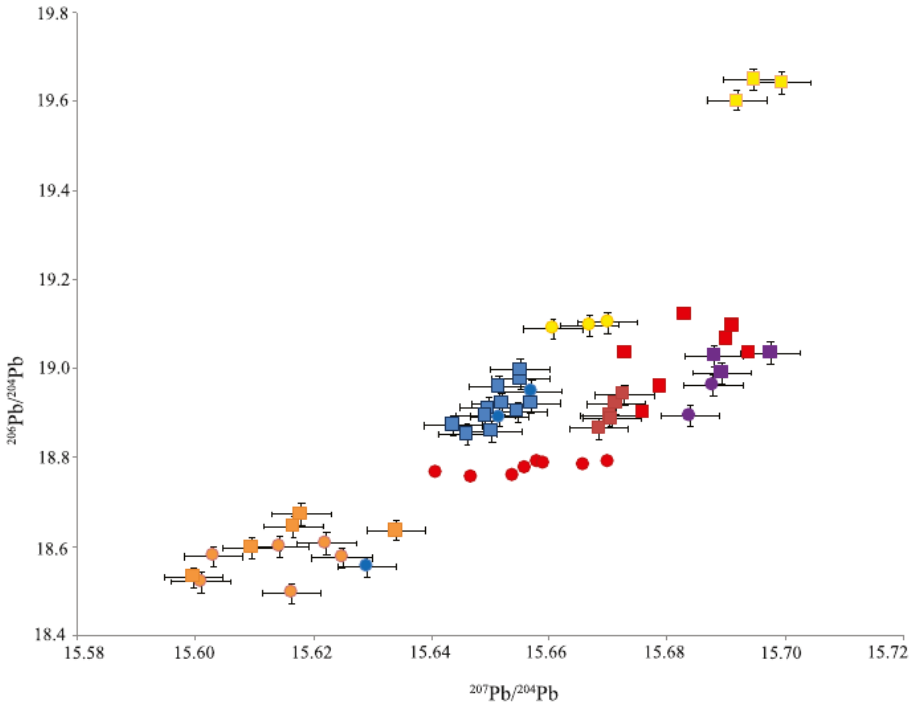

Figure 2. Comparison of bulk versus detrital fractions Pb isotope ratios of the same sample for source regions. Squares represent the bulk sediment, while circles are the detrital fraction isolated through sequential leaching. As no bulk sediment was available for the Chinese loess samples, both the Chinese bulk and detrital fractions from Jones et al. (2000) are shown in red for comparison purposes.

For the core-top detrital samples, $^{207}Pb/^{204}Pb$ ratios vary from 15.59 to 15.68, with most samples, particularly in the EEP, clustering around 15.63–15.64 (Table S2 and Figure 3). The least radiogenic ratios are generally located near coastal settings, particularly near Alaska and Central America. Conversely, the most radiogenic samples are located north of the equator at 140°W, as well as at open-ocean locations in the northwestern Pacific. These trends are also generally observed also in $^{206}Pb/^{204}Pb$ and $^{208}Pb/^{204}Pb$ ratios.

Downcore samples from PC72 (Table S4 and Figure 4) show slightly different trends with depth for each Pb isotopic ratio. The samples show an average value of ~18.85 for $^{206}Pb/^{204}Pb$, 15.66 for $^{207}Pb/^{204}Pb$, and 38.9 for $^{208}Pb/^{204}Pb$. Less radiogenic Pb isotopic ratios are noted, however, at the end of Marine Isotope Stage (MIS) 5c (87 ka), MIS 4 (63 ka), and a large excursion toward less radiogenic values during MIS 2 (25–14 ka). Within MIS2, all three ratios show a trend toward less radiogenic values at the start of MIS 2, though the least radiogenic values for each of the ratios occur at different times within MIS 2. Specifically, $^{206}Pb/^{204}Pb$ ratios are least radiogenic at 14.7 ka, $^{207}Pb/^{204}Pb$ are least radiogenic at 24.8 ka and thereafter gradually rise, while $^{208}Pb/^{204}Pb$ ratios remain low for the duration of MIS2

4. Discussion

4.1. Impact of Anthropogenic Contamination on Core-Top Data

Anthropogenic lead contamination of samples is a concern for any Pb isotopic study. To understand if samples from this and previous studies have been impacted, the composition of modern contamination is compared to our data set. While no present-day seawater Pb isotope records exist for the EEP, surface and depth profiles collected in 1979 (Flegal et al., 1984) and 2002 (Gallon et al., 2011; Zurbrick et al., 2017) have been reported for regions in the central and northwest Pacific, along with values for the Western Philippine Sea collected in 2014 (Chien et al., 2017). Of the surface seawater samples reported in Flegal et al. (1984), the sample at 2°N, 150°W is the closest sample to the ITCZ (1.176 $^{206}Pb/^{207}Pb$ 2.4318 $^{208}Pb/^{207}Pb$), while the sample at 15°S, 150°W (1.176 $^{206}Pb/^{207}Pb$, 2.443 $^{208}Pb/^{207}Pb$) is likely the most indicative of seawater

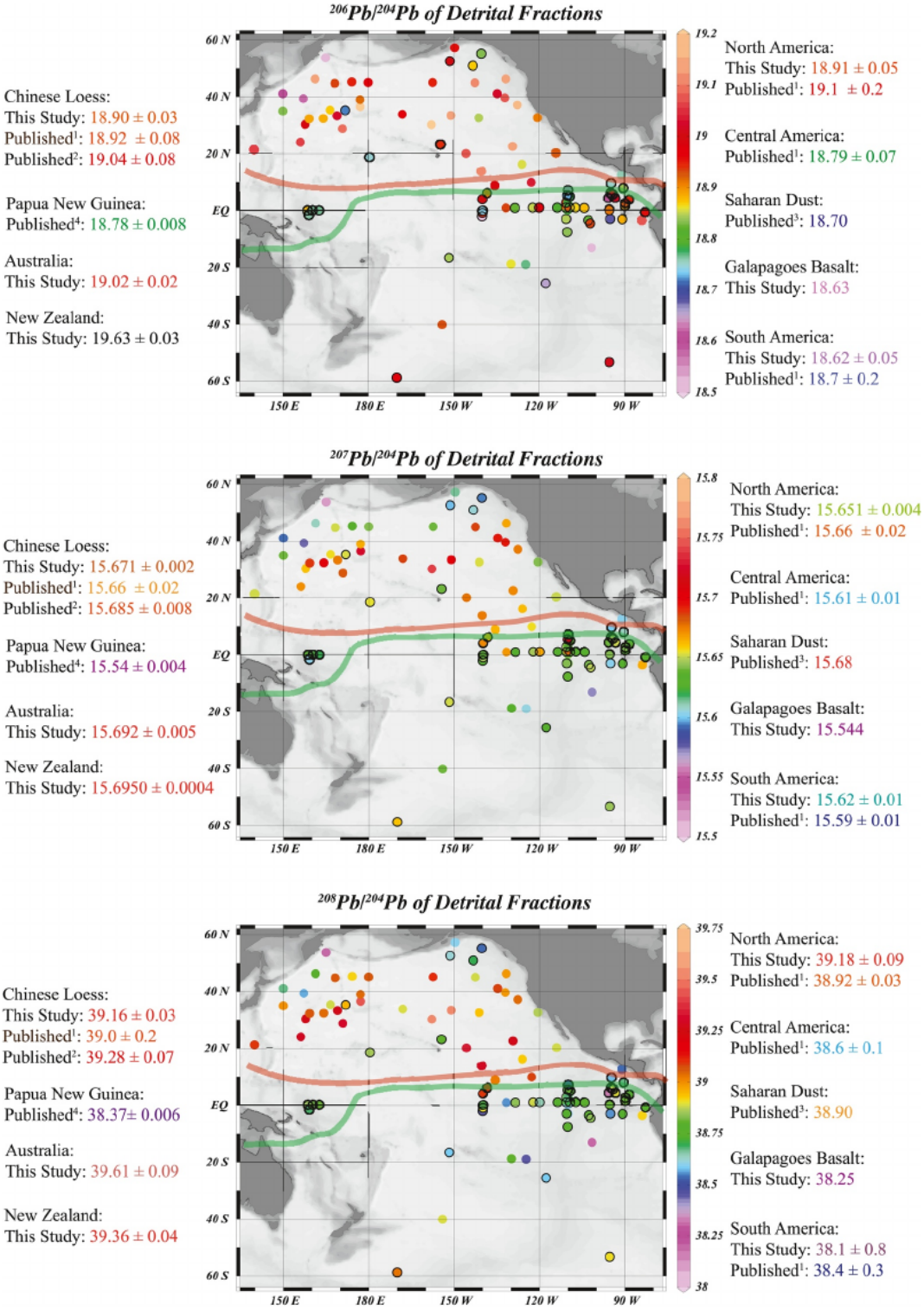

Figure 3. $^{206}Pb/^{204}Pb$, $^{207}Pb/^{204}Pb$, and $^{208}Pb/^{204}Pb$ results from core-top sediment detrital fractions across the Pacific Ocean measured for this study (outlined in dark circles) and published data (Godfrey, 2002; Hyeong et al., 2011; Jones et al., 2000; Pettke et al., 2000; Stancin et al., 2006, 2008, Xie & Marcantonio, 2012). Warmer colors represent more radiogenic ratios, and cooler colors less radiogenic ratios. Results for source regions are listed on the figure. [1]Published results from Stancin et al. (2006) calculated from analysis of core-top data; [2]Published ratios measured on the silicate (detrital) fraction of Chinese loess by Jones et al. (2000); [3]Published results of preanthropogenic Saharan dust compiled by Abouchami and Zabel (2003); [3]Published results for Papua New Guinea from Park et al. (2010). ITCZ summer (red) and winter (green) from Liu et al. (2015). ITCZ, Intertropical Convergence Zone.

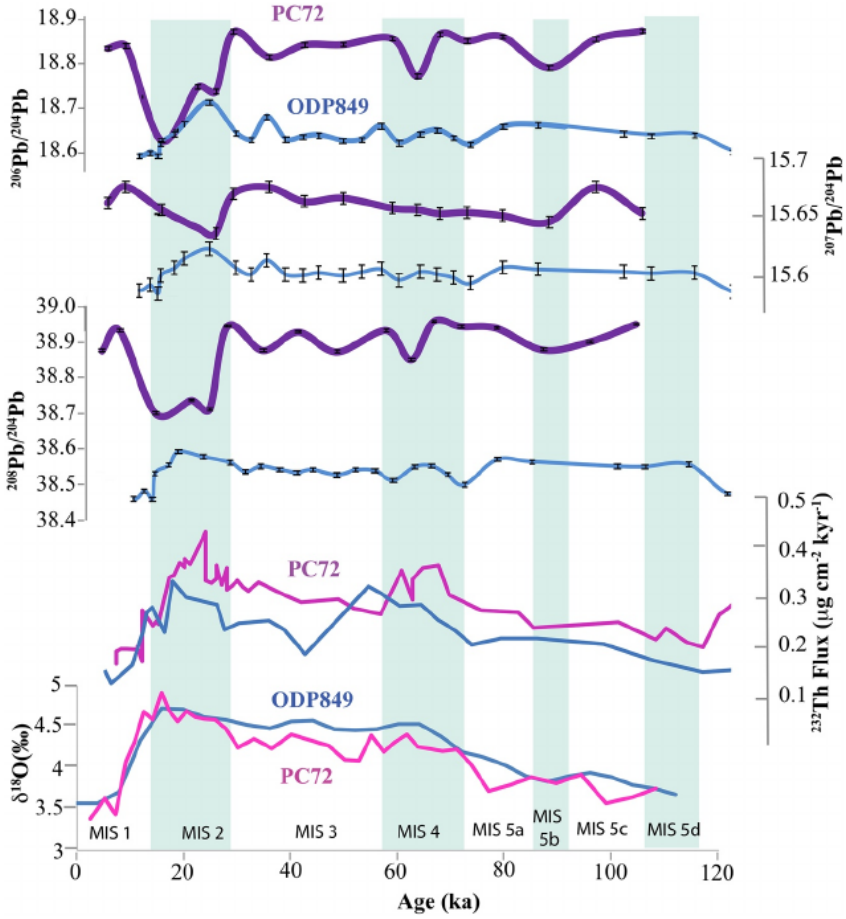

Figure 4. Downcore records of $^{206}Pb/^{204}Pb$, $^{206}Pb/^{204}Pb$, and $^{206}Pb/^{204}Pb$ PC72 (0.1°N, 139.4°W, purple, this study) and ODP Site 849 (110.5°W, 0.2°N, blue, Pichat et al., 2014). If no error bars are shown, the error (2sigma) is less than the symbol. ^{232}Th results (Winckler et al., 2008) for PC72 and ODP849 provide dust flux reconstructions. The oxygen isotope curves for PC72 (Mix et al., 1995) and ODP849 (McGee et al., 2007) are shown for climatic comparison.

influenced by southern source anthropogenic contamination. Additionally, the most eastern samples of Gallon et al., (2011) at 26.65°N, 152.06°W (1.164 $^{206}Pb/^{207}Pb$, 2.448 $^{208}Pb/^{207}Pb$) likely capture seawater influenced by northern sourced anthropogenic Pb such as North America. These seawater values generally correspond to the Pb isotope composition of modern dust, shown in Figure 5.

Pacific Ocean water depth profiles are consistent with limited anthropogenic Pb reaching the seafloor (Wu et al., 2010; Zurbrick et al., 2017), with anthropogenic Pb input declining sharply with distance from Asia (Zurbrick et al., 2017). Additionally, a compilation of modern aerosol values in Zurbrick et al. (2017) show that the Pb isotopes of aerosols Pb generally matches the surface seawater dissolved Pb isotope ratios and are different from the core-top samples in this study. These values for anthropogenic contamination can then be compared to sediment results. Overall, it appears that any anthropogenic Pb influence on core-top Pb isotopes or source region samples we present is likely limited. Any sample suspected of contamination based on its isotopic composition was removed from further discussion.

4.2. Pacific Ocean Core-Top Pb Data Compilation

4.2.1. Core-Top Samples—North and South Pacific

We observe that Pb isotope values for the detrital fraction in core-top samples from the North Pacific and those from the South Pacific differ, consistent with the known dust sources and the ITCZ location (Figure 3). The core-top samples in the North Pacific are more radiogenic (displayed as warmer colors in Figure 3) than

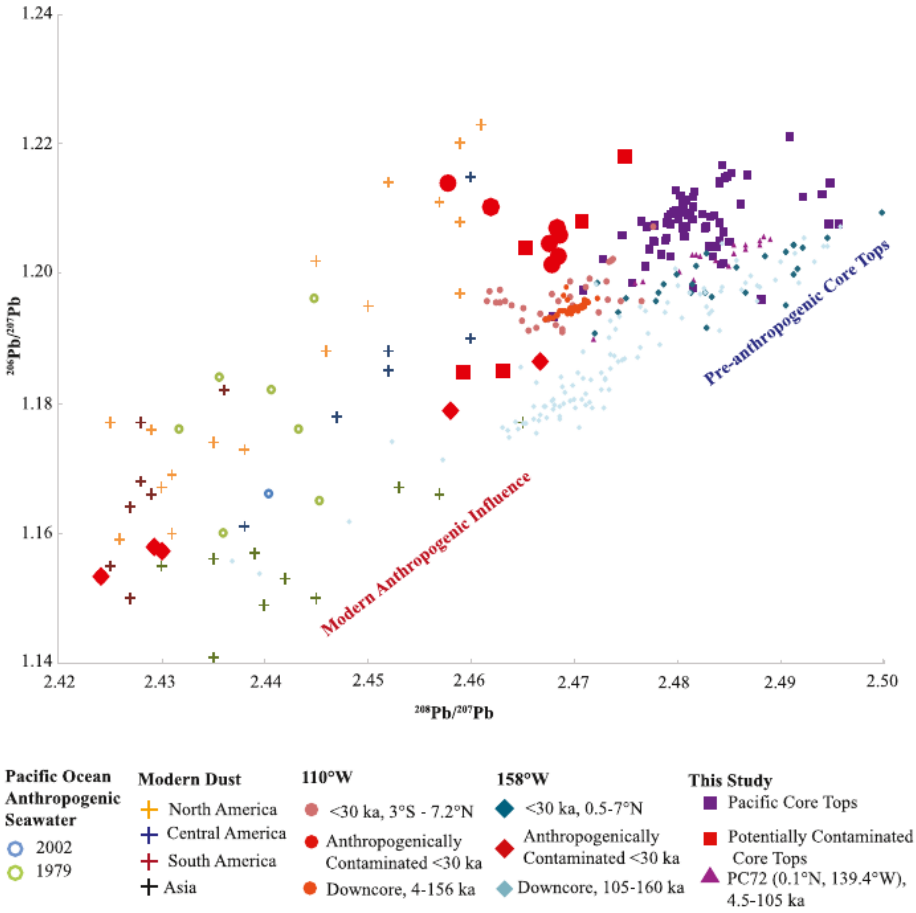

Figure 5. Pb isotope samples from core-top and downcore sediments in comparison to likely anthropogenic influence. Pacific Ocean anthropogenic seawater values are from 1979 (Flegal et al., 1984) and 2002 (Gallon et al., 2011; Zurbrick et al., 2017). Modern dust values are from Bollhöfer and Rosman (2000, 2001) for the Southern and Northern Hemisphere samples, respectively. Sediment samples from 110W are from Xie and Marcantonio (2012) (<30 ka) and Pichat et al. (2014) (downcore), while samples from 158°W are from Reimi et al. (2016) (<30 ka) and Reimi et al. (2019) (105–160 ka). Samples in red are core-top samples presumed to be anthropogenically contaminated.

samples from the equatorial and eastern Pacific, with the most radiogenic samples being in the western North Pacific consistent with the decrease in the fraction of Chinese loess with distance from source, as previously suggested by Jones et al. (2000). This is most clearly illustrated in the $^{207}Pb/^{204}Pb$ and $^{208}Pb/^{204}Pb$ ratios.

Some core-top samples, particularly near Hawaii and Alaska, are less radiogenic than most other samples from the North Pacific ($^{207}Pb/^{204}Pb$ isotopic composition ~15.64). This may reflect local influences. Hawaiian volcanic debris (average $^{207}Pb/^{204}Pb$ isotopic composition ~15.47, Abouchami et al., 2000; Marske et al., 2007; among others) likely contributes to the nearby core-top sample (23.2°N, 254.45°W). The less radiogenic core-top Pb isotopes (15.59–15.61 $^{207}Pb/^{204}Pb$) near Alaska are consistent with published detrital data from this region (Horikawa et al., 2015; Jones et al., 2000) and may include volcanic and/or fluvial material from continental Alaska and the Aleutian islands, which have an average $^{207}Pb/^{204}Pb$ ratio of ~15.56 (Chang et al., 2009; Greene et al., 2006). Similarly, we can attribute the less radiogenic Pb in the far western equatorial Pacific (~160°E) to local volcanic sources, such as Java, Indonesia, which has a $^{207}Pb/^{204}Pb$ ratio of ~15.6 (McDermott & Hawkesworth, 1991). These results, in combination with published detrital data from samples near Japan and the northernmost Pacific, point toward regional, less radiogenic volcanic influences affecting areas proximal to land in the Pacific (ring of fire).

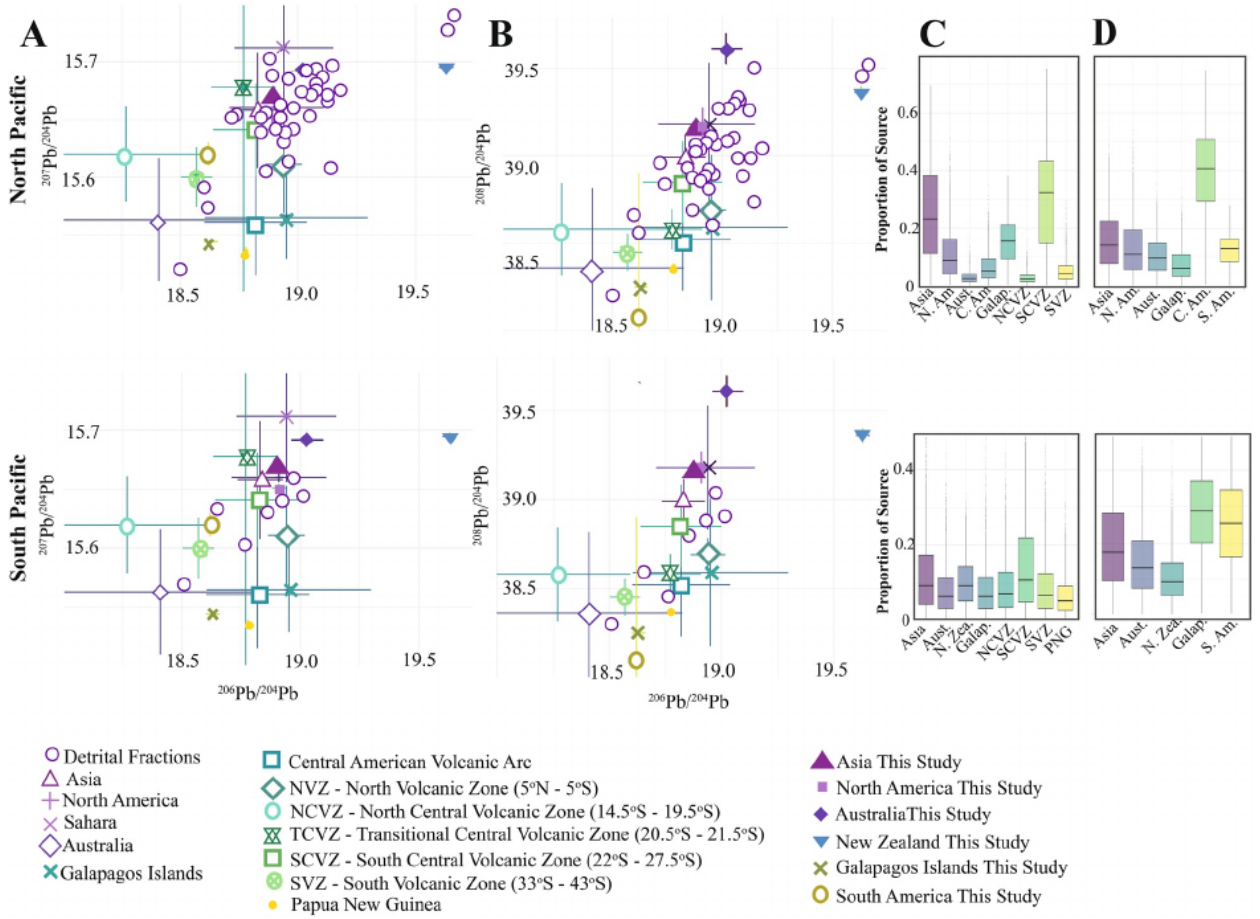

Figure 6. Detrital fractions and source area comparisons for five regions across the Pacific Ocean. Columns A and (b) Detrital fractions (open circles) for each region with mean source area data from Pichat et al. (2014) and Park et al. (2010) and this study. Columns C and (d) Whisker plots show the likely proportion of each source using a three-isotope mixing model with only likely sources. Column C uses source end member and standard deviation values from Pichat et al. (2014), while Column D uses the source end members from this study.

The few samples analyzed in this study from the south Pacific show more radiogenic ratios (15.63–15.66 $^{207}Pb/^{204}Pb$) in the south Pacific compared to the north Pacific Ocean, consistent with the more radiogenic signature of New Zealand and Australian loess observed in this study. This radiogenic signature is complicated by the less radiogenic South American samples, although the influence from that region to the open-ocean South Pacific is likely limited (Li et al., 2008).

While general trends in dominant dust source regions can be observed from a visual analysis, multiple sources are likely to contribute dust at each site. The contributions of each source, and the potential to identify less prevalent source contributions, require additional techniques such as source apportion mixing models. When our data for the various regions are used in an isotope mixing model (Figure 6), the nonuniqueness of each potential source is highlighted. When all potential sources used in the literature (compiled in Pichat et al. [2014] and Höfig et al. [2016]) are included in our isotope cross-plots (Figure 6, columns A and B), we see that the Pb isotopic overlap between end member source samples makes differentiation challenging. To simplify, only likely source regions were included in the isotope mixing models, with column C in Figure 6 utilizing the literature data and column D in Figure 6 source area results from this study.

For the North Pacific, mixing models using published data show that Asian and North American sources predominate. This is consistent with our knowledge of wind patterns and observations from the spatial distribution shown in Figure 3. As expected, few of the southern sources cross the ITCZ. The mixing models results differ, however, depending on source region values used. While results from previously published data attribute the greatest source probability to North America and Asia, using results obtained in this study

we attribute a higher source region probability to Central American sources. This highlights the sensitivity of mixing models to both source region values and the number of sources considered.

This difference illustrates the challenges of using Pb isotopes as a dust source tracer. Each source region data compilation has its limitations. The published data set is composed primarily of bulk rock material which may not be representative of dust while data from this study are limited in number and not comprehensive. While the differences between the Pb isotope values used in the literature and those produced and used in this study vary only slightly, mixing model results show sizable shift in the proposed influence of the difference sources.

For the Southern Pacific, model results for both published source data and data from this study do not identify a conclusive source. Indeed, the probability of contribution from Asian versus Australian sources is very similar, although the ITCZ likely impedes significant Asian dust transport to this region (Kienast et al., 2016). Again, the isotopic overlap of Pb in likely sources makes clear source determinations difficult when Pb isotopes are used as a sole indicator.

While overall differences are observed in Northern and Southern Pacific samples, the wide range in Pb isotopes of both the detrital sample data and data from potential sources makes unique source region identifications challenging. We note that in addition to source differences between the North and South Pacific, spatial patterns, such as proximity to unique local (i.e., Hawaii or Aleutian Islands) sources, play a role. Isotope mixing models highlight the difficulty of distinguishing sources when the source isotopic ranges are large and not unique, the number of potential sources is large, and/or when relatively small differences within end members result in large differences in the mixing models source probability results.

Finally, the source region values, from both this study and others, are not radiogenic enough to fully characterize sources of all samples. In particular, a few samples in the North Pacific have $^{206}Pb/^{204}Pb$ isotope values greater than 19 which would suggest New Zealand as a predominant source, a scenario that seems unlikely given known dust transport processes. Other workers have also found a handful of samples with values more radiogenic than those defined by expected source regions (Reimi et al., 2019). Overall, while the known general dust source trends are supported by isotopic results, some details regarding source identification for all sediment samples remains elusive.

4.2.2. Core-Top Samples—Eastern Equatorial Pacific

Given that the location of the ITCZ is presumed to have a prevailing influence on the sources of dust reaching the EEP and that the ITCZ location is known to vary both seasonally and over longer-term climate cycles (Liu et al., 2015), we have further focused our study on samples from the EEP. Although the large-scale source signals are captured in the EEP as noted above, on a regional to local scale significant variability was observed in Pb isotope signatures of the detrital fractions among cores in the EEP, consistent with other studies (Reimi et al., 2016; Xie & Marcantonio, 2012).

Because the location of the ITCZ creates a boundary between Northern and Southern hemisphere dust sources, we should be able to differentiate sources north and south of the ITCZ in the EEP, particularly when viewing results spatially at any given time interval (Figure 3). As expected, the Pb isotope values of samples lying north of the ITCZ, for example, the northern most samples at 140°W, cluster closer to the northern hemisphere sources. South of the ITCZ South America is a dominant dust source to the EEP, particularly at longitudes east of ~100°W (Saukel et al., 2011). This is reflected in the Pb isotopic signatures in our samples, although clearly observed only when using the published bulk source isotope values and not to those from this study (Figure 7). Core-top samples from the EEP are isotopically most similar to the published South and Central American source regions with an overall east-west gradient showing reduced influence of this source to the west (Figure 3). When the source signatures from this study are used, Central American sources predominate east of 120°W (Figure 7).

Across the broader EEP (Figure 3), the most radiogenic samples predominantly occur to the west, with less radiogenic values at longitudes east of 110°W, particularly for $^{207}Pb/^{204}Pb$ and $^{208}Pb/^{204}Pb$ likely due to the influence of Andean volcanism. The east-west trend is consistent with the increasing influence of Chinese loess in the west Pacific and increased influence of South and Central American sources in the eastern sector of the EEP.

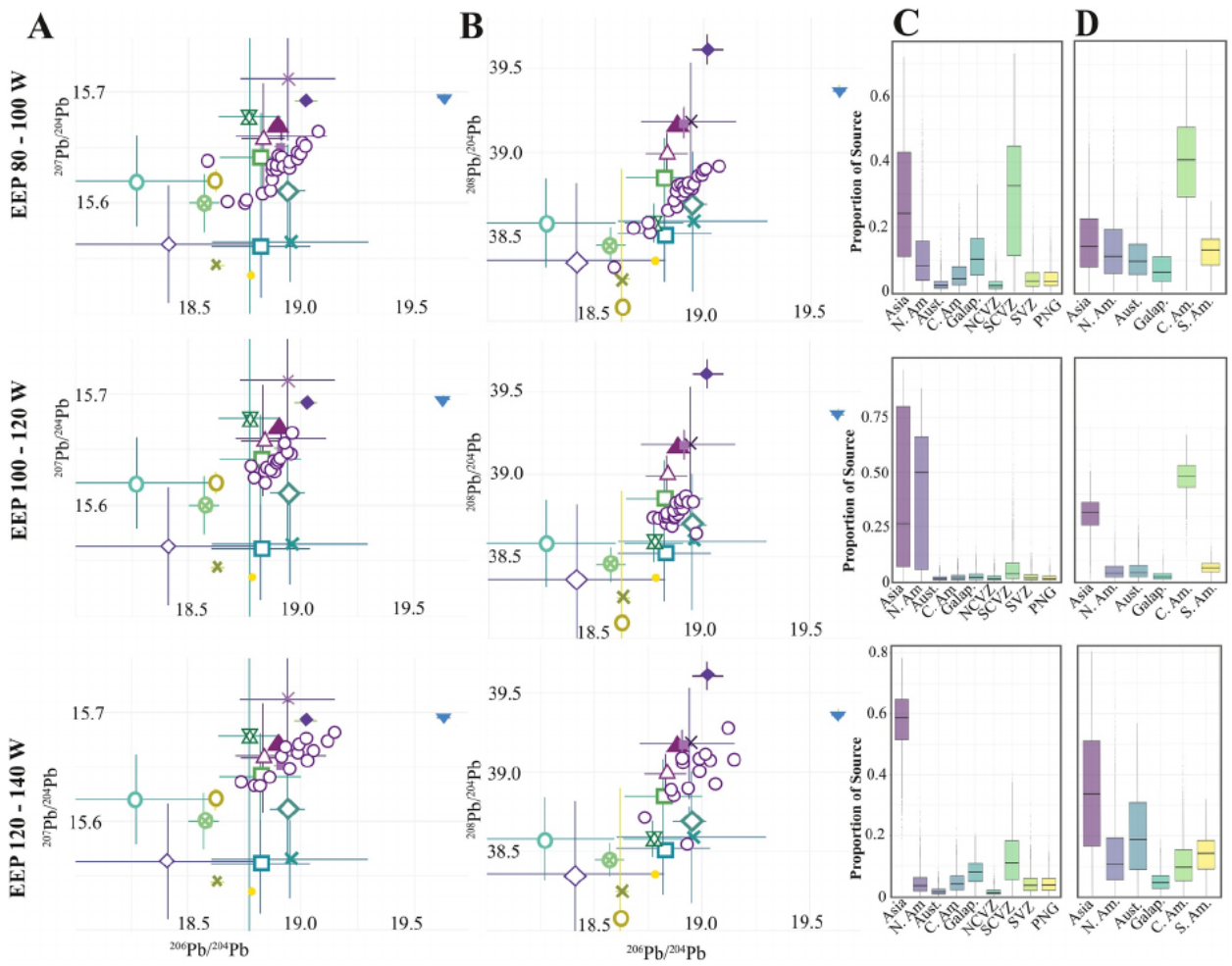

Figure 7. Detrital fractions and source area comparisons for five regions across the Pacific Ocean. See Figure 6 for legend and data sources.

When looking at samples collected along a transect or at locations within a degree from each other, considerable variability is apparent. For example, along ~140°W, with samples spanning from 6°N to 1°S, the difference between the maximum and minimum values were 0.41, 0.049, and 0.40 for $^{206}Pb/^{204}Pb$, $^{207}Pb/^{204}Pb$, and $^{208}Pb/^{204}Pb$, respectively (Figure 3). These differences, seen across transects in the EEP, reinforce the need to better constrain sources of variability. Intermittent small-scale changes in dust sources over time and different sedimentation, bioturbation rates and sediment focusing may result in high variability between relatively adjacent cores even when using identical sample processing procedures.

It was not possible to precisely date each sample for this study, and previously published ages are available for only a handful of cores. Specifically, the role of bioturbation in integrating different age windows of sediment deposition is unknown. Therefore, if the samples represent a wide age range, variability may correspond to temporal regional shifts in dust sources and abundance. Downcore studies, with well-dated cores, provide more promise to understanding temporal changes in dust deposition patterns.

Finally, when the likely source regions are considered within the isotope mixing model, differences between previously published source signatures and source signatures obtained in this study are observed (Figure 7). All model outputs show a sizable component of Asian dust as expected. For the published source region data from Stancin et al. (2006) and Reimi et al. (2019) model results attribute a sizable component of the sediment detrital fraction Pb to the South-Central Volcanic Zone. Even though the South American sample in this study was from a roughly similar location regionally, it was not a dominant source in the mixing model. Instead, Central American sediment was a more prominent source. Interestingly, the probability of

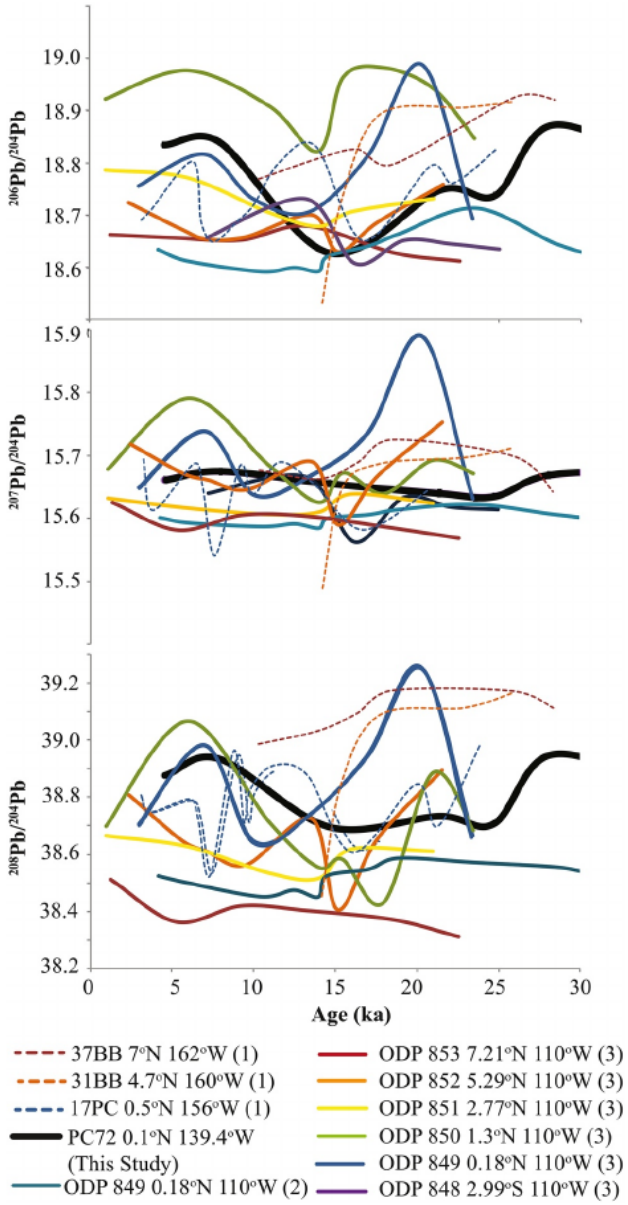

Figure 8. Pb isotope ratio downcore records for the Equatorial Pacific. Samples from ~160°W are shown in dashed and 110°W in solid lines, with warmer shades for more northern locations. Data sources are (1) Reimi et al. (2016), (2) Pichat et al. (2014), and (3) Xie and Marcantonio (2012). Results from PC72 at 140°W are from this study.

North American sources was lowest in between 100°W and 120°W (Figure 7). Again, the lack of a known radiogenic source end member limits the accuracy of any mixing model.

The impact of small differences in source area values, and even the selection of "likely" source areas, has the potential to significantly alter mixing model results. While the clear importance of Asian dust throughout the EEP remained in any simulation, the use of the detrital fraction of samples from the various source regions increased the potential contribution of Australian and South American sources in the samples from 120°W to 140°W. This exercise highlights the importance of careful consideration of which sediment fractions are influencing sediment isotopic signatures.

The large difference in Pb isotope ratios from spatially adjacent cores at any given time, particularly cores that are well dated, show the sensitivity of Pb to local changes in dust flux or suggest other nondust input related local effects as discussed above for the core tops. The variability in the Pb isotope data also suggests the possibility of considerable local fluctuations in dust input and hence uncertainty in age assignment can perhaps explain at least some of the differences observed in the EEP core-top samples.

4.3. Downcore Trends in EEP Pb Isotopic Ratios

Multiple downcore records of Pb isotope ratios have been previously measured in the Equatorial Pacific. Existing records have focused on two locations-a N-S transect from 0.5°N to 7°N between 156°W and 162°W (Reimi et al., 2016, 2019) and between 3°S and 7°N along 110°W, including ODP849 (Pichat et al., 2014; Xie & Marcantonio., 2012). The records from ODP849 are shown in Figure 4, along with our record from PC72 at 140°W.

Each downcore data set compared here was prepared with slightly different separation techniques, which has the potential to result in differences caused by sample treatment. However, studies have generally shown that most of the Pb in open-ocean sediments is found in the residue/detrital fraction (70.1%–91.6% in Pichat et al., 2014). Additionally, Pichat et al. (2014) have shown that in ocean sediment samples the bulk and detrital fractions are similar within analytical error, supporting their usage of bulk sediment for downcore analysis. Therefore, interpretations that are based on trends rather than absolute values between datasets should be valid.

The compilation of results from each study (Pichat et al., 2014; Reimi et al., 2016; Xie & Marcantonio, 2012) shows inconsistent trends for samples collected in the same region along a transect, particularly samples from the last 30 kyr (Figure 8). There is also no similarity within sites on either side of the ITCZ or clear consistent trends along the N-S transect for either 160°W or 110°W. We would expect, for example, that the northernmost sites along each of the transects would have the highest contribution of Pb from more radiogenic northern dust sources. However, the northernmost sample at 160°W is among the most radiogenic while the sample at a similar latitude at 110°W is among the least radiogenic (Figure 8). This may suggest that source contributions over time at each site varied independently, resulting in differences in trends within proximal regions or that samples at each time interval represent different integrated time slices as discussed in Section 4.2.2.

The ranges of values observed, both within a single core over time and during a specific time interval in different cores along transects, is similar or greater than that observed in core-top sediments from the EEP. The

core-top sediments from the EEP have a range of 0.40 for $^{208}Pb/^{204}Pb$ ratios. Comparatively, the downcore range for PC72 from this study for $^{208}Pb/^{204}Pb$ is 0.26, while the published range for $^{208}Pb/^{204}Pb$ at the equatorial sites at 110°W and 160°W is 0.60 and 0.42, respectively (Xie & Marcantonio, 2012). Further expanding the comparison, when all downcore samples from the last 30 kyr are considered from the transects at 110°W and 160°W, the range is 0.93 and 0.71 $^{208}Pb/^{204}Pb$, respectively (Figure 8).

Comparing the longer-term record from PC72 (this study) to that from ODP849, located 30° to the east (Pichat et al., 2014), we see that generally samples from the central equatorial Pacific are more radiogenic, hence likely have a greater influence of northern sourced dust, than samples to the east (Figure 4). Samples from ODP849 are more similar to South American sources. Given the similar latitude of ODP849 and PC72, it is likely that the two locations remained on the same, that is, southern, side of the ITCZ throughout this time interval. However, the Pb isotope ratios during MIS 2, between 29 and 14 ka during the LGM and deglacial, have an antithetic trend between the two cores. PC72 during MIS2 records less radiogenic isotopic ratios, trending toward more southern sources, and ODP849 records more radiogenic isotopic ratios, trending toward more northern sources such that the sites become more similar to each other.

Multiple processes could explain both the changes in the Pb isotopic ratios over time in a single core and differences between cores at any given time. To constrain changes in dust flux it is useful to consider 232 thorium excess ($^{232}Th_{excess}$), a proxy for dust deposition. A relation between $^{232}Th_{excess}$ dust flux and the $\delta^{18}O$ climate records has been previously noted (Jacobel et al., 2017; Winckler et al., 2008) and suggest an increased dust flux during glacial intervals. The $^{232}Th_{excess}$ record shows an overall increase leading into the LGM. Such an increase without change in source would not impact the Pb isotope record, however, we see changes in the Pb isotopic records for both PC72 and ODP849 with the differences between sites decreasing. This may indicate a new dust source contributing to the system at both sites. In this case, this source is expected to have an isotopic signature that is less radiogenic than the North American-Asian end members but more radiogenic than the South and Central American sources. Alternatively, an increase in the relative contribution from an existing source with such an intermediate signature could also explain the trend. Potential sources for this include some subregions of South America, such as the Transitional Central Volcanic Zone (20.5°S–21.5°S), though no one source is definitive.

The possibility remains that the ITCZ is not as effective of a dust barrier as generally proposed, particularly during glacial times. This would result in a greater mixing of dust sources, contributing to the convergence of Pb isotope values at ~20 ka in the two cores considered here. Indeed, McGee et al. (2007) considered dust flux along a N-S transect from 7°N to 3°S in the EEP (including ODP849), showing a reduced gradient of dust across the equator during glacial times, potentially from a weaker ITCZ. Additionally, this theory provides an explanation for the considerable variability observed in the compiled 30 ka record (Figure 8), i.e., a greater and more variable degree of mixing of northern and southern sourced dust.

The records presented here do not provide a definitive link between dust inputs and ITCZ dynamics but highlight the complexity of using Pb isotopes for high-resolution dust source reconstructions. With difficulty in constraining dust sources and isotopic ambiguity between likely sources, Pb isotopes must be coupled with other isotope systems, such as Nd, Sr, and/or Hf isotopes, for more definitive reconstructions (Grousset and Biscayne, 2005; Trudgill et al., 2020; Xie & Marcantonio, 2012).

Finally, circulation changes cannot be excluded as driver for the variability observed at 140°W. As Ziegler et al. (2008) estimated a maximum contribution of ~25% of material from Papua New Guinea to core PC72, contributions of detrital fractions via the Equatorial Undercurrent are possible. Given the relatively less radiogenic values for Papua New Guinea sediment (Kennedy et al., 1990; Park et al., 2010), the lower Pb isotope ratios in core PC72 during cooler intervals may result from an increase in the Equatorial Undercurrent strength and/or greater erosion of Papua New Guinea sediments. While our core-top isotope mixing model does not show a sizable influence of Papua New Guinea sediments to the EEP, further work is needed to understand the role of Equatorial Undercurrent transport to this region.

4.4. Methodological Influences on Detrital Particle Pb Isotopes

Incomplete removal of Pb from nonterrigenous constituents in the sediment, including biogenic silica, authigenic clays, refractory authigenic minerals, and volcanic minerals, have the potential to influence the

Pb isotope ratio of the samples. This is evident from the differences seen in results obtained using different leaching procedures when applied to the same core-top samples (Hyeong et al., 2011) and the differences in average source values between published data and this study which used different sample treatments prior to analysis (Figures 5 and 6).

The question of isotopic differences among distinct mineralogical phases within a sample has been considered for both marine sediments and terrigenous dust source regions. For example, for Pacific Ocean sediments, Pichat et al. (2014) considered the issue of divergent Pb isotopic ratios between the insoluble residue and bulk sediment fractions. Seven samples from ODP849 were analyzed for some combination of bulk, leachate, and residue after a range of acetic acid and hydroxylamine hydrochloride leaches. Each of these samples had a $^{206}Pb/^{204}Pb$ and $^{208}Pb/^{204}Pb$ in the residue fraction within error of the bulk fraction, with the residue fraction accounting for 70.1–91.6% of the total Pb (Pichat et al., 2014). This however may not be the case for other oceanic sites and most likely not for source region samples. The mineralogical composition of source regions generally differs from ocean sediment, with implications to the distribution of Pb in different fractions of the source sample. Existing compilations by Pichat et al. (2014) and Höfig et al. (2016) were based upon bulk measurements of predominantly igneous rocks material. Bulk source samples of heterogeneous sedimentary rocks and, more specifically topsoil, likely contain phases such as carbonates and organic matter. Indeed, Yokoo et al. (2004) analyzed sequential leachates from loess and desert sand from the Chinese Loess Plateau, isolating evaporite, calcite, phosphate, and insoluble phases. Each leachate fraction had distinct $^{87}Sr/^{86}Sr$ ratios. While Pb isotopes were not included, it was clear that consistency between measured fraction(s) of source region samples and the sample representing the dust fraction is needed if we are to use source region values to reconstruct dust sources.

Bulk and detrital fractions from four broad source regions, including New Zealand, Australia, South America, and North America show that some samples had similar isotope ratios for both bulk and detrital fractions, but this was not universally the case. Samples from New Zealand, Australia, and the published results from China show differences between the isotope ratios of the bulk source region sample and the detrital fraction of the sediment samples, while in North and South American samples bulk and detrital fractions were generally similar. Where the bulk and detrital fractions differ, i.e., New Zealand, Australia, and China, the detrital fraction has a less radiogenic $^{207}Pb/^{204}Pb$ and $^{208}Pb/^{204}Pb$ ratio than the bulk sediment (Figure 2).

While this study contained only a limited number of samples, our results suggest that there are implications for the use of Pb isotopes in bulk rocks as representative end members for aeolian materials accumulating in the sediment. The agreement in Pb isotopes between the potential source region signature and the detrital fraction in sediments depends on the mineralogical composition of the source material and the chemical preparation treatment used to characterize the samples. As such, caution should be taken in terms of using bulk source material data as an end member representing the delivered and deposited dust composition. Additionally, a lack of methodological consistency for isolating the detrital fraction from sediments may complicate comparison between studies. As we have observed in the mixing model results, small differences in assigned source region values, such as those that can result from using bulk versus the isolated detrital fractions of source regions, can significantly impact dust source reconstructions.

5. Conclusion

In this study, we examined the utility of Pb isotopes for tracing dust deposition sources across the Pacific, with an emphasis on the EEP. We observed that ocean-scale trends, such as a general differentiation of Pb isotopic ratios north and south of the ITCZ, remain clear. However, a relatively large difference in Pb isotopic data in proximal cores was observed in this and other studies. We focused on understanding if these differences result from dust delivery from different source regions, anthropogenic contamination of samples, poor age control contributing to differences in signal integration, and/or changes in sedimentary components analyzed over time.

Overall, it is likely that the heterogeneity of dust sources to the EEP, combined with changes to the location and/or efficiency of the ITCZ to impede mixing of northern and southern dust, result in inconsistencies in Pb isotope ratios between adjacent cores. Downcore records from PC72 and ODP849 show changes on glacial/interglacial scales, highlighting the role of climate in dust delivery. As such, poor age control may result

in different cores capturing different climatic, and therefore dust depositional, environments. Core-top samples have Pb isotopic ratios more similar to downcore records than to modern dust and seawater, suggesting a limited role of anthropogenic contamination. Finally, we note that differences between bulk and detrital phases for many source regions may complicate interpretation and it is important for further studies to better constrain source regions based on specific minerals analyzed, possibly even utilizing single mineral signatures. Overall, while basin-scale source regions may be identified based on Pb isotopes, regional-scale Pb isotope results are variable both spatially and temporally making the determination of ITCZ location and movement difficult using only Pb isotopes.

Data Availability Statement

All data used in this study are contained within the references and tables and have been uploaded to the Zenodo data base http://doi.org/10.5281/zenodo.4440228.

Acknowledgments
Daniel R. Muhs and Jeffrey S. Pigati provided source region samples for North America and the Atacama Desert, respectively, along with enlightening comments on the manuscript. Christopher Moy collected samples from the New Zealand region. The Oregon State and Scripps Institute of Oceanography core repositories provided ocean sediment samples for this study. Rob Franks provided critical assistance with both the ICP-MS and MC-ICP-MS at the University of California at Santa Cruz. Cheryl Zubrick was a wonderful resource for instrument troubleshooting on the MC-ICP-MS. Funding for this work was in part provided by NSF CAREER Grant OCE-0449732 and NSF-OCE Grant 0850467 to Adina Paytan and a Schlanger Ocean Drilling Fellowship to Andrea M. Erhardt. We thank R. Xie, an anonymous reviewer, and editor U. Röhl for the constructive feedback.

References

Abouchami, A., & Zabel, M. (2003). Climate forcing of the Pb isotope record of terrigenous input into the Equatorial Atlantic. *Earth and Planetary Science Letters*, *213*, 221–234.

Abouchami, W., Galer, S. J. G., & Hofmann, A. W. (2000). High precision lead isotope systematics of lavas from the Hawaiian Scientific Drilling Project. *Chemical Geology*, *169*, 187–209. https://doi.org/10.1016/s0009-2541(00)00328-4

Anderson, R. F., Cheng, H., Edwards, R. L., Fleisher, M. Q., Hayes, C. T., Huang, K.-F., et al. (2016). How well can we quantify dust deposition to the ocean? *Philosophical Transactions of the Royal Society A*, *374*, 20150285. https://doi.org/10.1098/rsta.2015.0285

Arimoto, R. (2001). Eolian dust and climate: relationships to sources, tropospheric chemistry, transport and deposition. *Earth-Science Reviews*, *54*(1-3), 29–42.

Bayon, G., Douglas, G. B., Denton, G. J., Monin, L., De Deckker, P., Bermell, S., et al. (2020). Preferential riverine export of fine volcanogenic particles to the southeast Australian margin. *Frontiers in Marine Science*, *7*, 89. https://doi.org/10.3389/fmars.2020.00089

Bollhöfer, A., & Rosman, K. J. R. (2000). Isotopic source signatures for atmospheric lead: The Southern Hemisphere. *Geochimica et Cosmochimica Acta*, *64*, 3251–3262. https://doi.org/10.1016/s0016-7037(00)00436-1

Bollhöfer, A., & Rosman, K. J. R. (2001). Isotopic source signatures for atmospheric lead: The Northern Hemisphere. *Geochimica et Cosmochimica Acta*, *65*, 1727–1740. https://doi.org/10.1016/s0016-7037(00)00630-x

Chang, J. M., Feeley, T. C., & Deraps, M. R. (2009). Petrogenesis of basaltic volcanic rocks from the Pribilof Islands, Alaska, by melting of metasomatically enriched depleted lithosphere, crystallization differentiation, and magma mixing. *Journal of Petrology*, *50*, 2249–2286. https://doi.org/10.1093/petrology/egp075

Chien, C.-T., Ho, T.-Y., Sanborn, M. E., Yin, Q.-Z., & Paytan, A. (2017). Lead concentrations and isotopic compositions in the Western Philippine Sea. *Marine Chemistry*, *189*, 10–16. https://doi.org/10.1016/j.marchem.2016.12.007

Chien, C.-T., Mackey, K. R. M., Dutkiewicz, S., Mahowald, N. M., Prospero, J. M., & Paytan, A. (2016). Effects of African dust deposition on phytoplankton in the western tropical Atlantic Ocean off Barbados. *Global Biogeochemical Cycles*, *30*, 716. https://doi.org/10.1002/2015GB005334

Flegal, A. R., Schaule, B. K., & Patterson, C. C. (1984). Stable isotopic ratios of lead in surface waters of the central Pacific. *Marine Chemistry 14*, 281–287. https://doi.org/10.1016/0304-4203(84)90048-3

Galer, S. J. G. (1999). Optimal double and triple spiking for high precision lead isotopic measurement. *Chemical Geology*, *157*, 255–274. https://doi.org/10.1016/s0009-2541(98)00203-4

Gallon, C., Aggarwal, J., & Flegal, A. R. (2008). Comparison of mass discrimination correction methods and sample introduction systems for the determination of lead isotopic composition using a multicollector inductively coupled plasma mass spectrometer. *Analytical Chemistry*, *80*, 8355–8363. https://doi.org/10.1021/ac800554k

Gallon, C., Ranville, M. A., Conaway, C. H., Landing, W. M., Buck, C. S., Morton, P. L., & Flegal, A. R. (2011). Asian industrial lead inputs to the North Pacific evidenced by lead concentrations and isotopic compositions in surface waters and aerosols. *Environmental Science & Technology*, *45*, 9874–9882. https://doi.org/10.1021/es2020428

Godfrey, L. V. (2002). Temporal changes in the lead isotopic composition of red clays: Comparison with ferromanganese crust records. *Chemical Geology*, *185*, 241–254. https://doi.org/10.1016/s0009-2541(01)00406-5

Greene, A. R., Debari, S. M., Kelemen, P. B., Blusztajn, J., & Clift, P. D. (2006). A detailed geochemical study of island arc crust: The Talkeetna Arc section, South-Central Alaska. *Journal of Petrology*, *47*, 1051–1093. https://doi.org/10.1093/petrology/egl002

Grousset, F. E., & Biscaye, P. E. (2005). Tracing dust sources and transport patterns using Sr, Nd and Pb isotopes. *Chemical Geology*, *222*, 149. https://doi.org/10.1016/j.chemgeo.2005.05.006

Gutjahr, M., Frank, M., Stirling, C. H., Klemm, V., van de Flierdt, T., & Halliday, A. N. (2007). Reliable extraction of a deepwater trace metal isotope signal from Fe-Mn oxyhydroxide coatings of marine sediments. *Chemical Geology*, *242*, 351–370. https://doi.org/10.1016/j.chemgeo.2007.03.021

Höfig, T. W., Hoernle, K., Hauff, F., & Frank, M. (2016). Hydrothermal versus active margin sediment supply to the eastern equatorial Pacific over the past 23 million years traced by radiogenic Pb isotopes: Paleoceanographic and paleoclimatic implications. *Geochimica et Cosmochimica Acta*, *190*, 213–238. https://doi.org/10.1016/j.gca.2016.05.003

Horikawa, K., Martin, E. E., Basak, C., Onodera, J., Seki, O., Sakamoto, T., et al. (2015). Pliocene cooling enhanced by flow of low-salinity Bering Sea water to the Arctic Ocean. *Nature Communications*, *6*, 7587. https://doi.org/10.1038/ncomms8587

Hyeong, K., Kim, J., Pettke, T., Yoo, C. M., & Hur, S.-D. (2011). Lead, Nd and Sr isotope records of pelagic dust: Source indication versus the effects of dust extraction procedures and authigenic mineral growth. *Chemical Geology*, *286*, 240–251

Jacobel, A. W., McManus, J. F., Anderson, R. F., & Winckler, G. (2017). Climate-related response of dust flux to the central equatorial Pacific over the past 150 kyr. *Earth and Planetary Science Letters*, *457*, 160–172. https://doi.org/10.1016/j.epsl.2016.09.042

Jacobson, A. D. (2004). Has the atmospheric supply of dissolved calcite dust to seawater influenced the evolution of marine87Sr/86Sr ratios over the past 2.5 million years? *Geochemistry, Geophysics, Geosystems*, *5*, Q12002. https://doi.org/10.1029/2004GC000750

Jones, C. E., Halliday, A. N., Rea, D. K., & Owen, R. M. (2000). Eolian inputs of lead to the North Pacific. *Geochimica et Cosmochimica Acta*, *64*, 1405–1416. https://doi.org/10.1016/s0016-7037(99)00439-1

Kalnay, E., Kanamitsu, M., Kistler, R., Collins, W., Deaven, D., Gandin, L., et al. (1996). The NCEP & NCAR 40-year reanalysis project. Bulletin of the American, American Meteorological Society, 77, 437–471.

Kamber, B. S., & Gladu, A. H. (2009). Comparison of Pb purification by anion-exchange resin methods and assessment of long-term reproducibility of Th/U/Pb Ratio measurements by quadrupole ICP-MS. *Geostandards and Geoanalytical Research*, *33*, 169–181. https://doi.org/10.1111/j.1751-908x.2009.00911.x

Kamenov, G. D., Mueller, P. A., & Perfit, M. R. (2004). Optimization of mixed Pb-Tl solutions for high precision isotopic analyses by MC-ICP-MS. *Journal of Analytical Atomic Spectrometry*, *19*, 1262–1267. https://doi.org/10.1039/b403222e

Kennedy, A. K., Hart, S. R., & Frey, F. A. (1990). Composition and isotopic constraints on the petrogenesis of alkaline arc lavas: Lihir Island, Papua New Guinea. *Journal of Geophysical Research*, *95*(B5), 6929–6942. https://doi.org/10.1029/jb095ib05p06929

Kienast, S. S., Winckler, G., Lippold, J., Albani, S., & Mahowald, N. M. (2016). Tracing dust input to the global ocean using thorium isotopes in marine sediments: ThoroMap. *Global Biogeochemical Cycles*, *30*(10), 1526–1541. https://doi.org/10.1002/2016GB005408

Li, F., Ginoux, P., & Ramaswamy, V. (2008). Distribution, transport, and deposition of mineral dust in the Southern Ocean and Antarctica: Contribution of major sources. *Journal of Geophysical Research*, *113*, D10207. https://doi.org/10.1029/2007JD009190

Liu, Y., Lo, L., Shi, Z., Wei, K.-Y., Chou, C.-J., Chen, Y.-C., et al. (2015). Obliquity pacing of the western Pacific Intertropical Convergence Zone over the past 282,000 years. *Nature Communications*, *6*, 10018. https://doi.org/10.1038/ncomms10018

Mackey, K. R. M., Buck, K. N., Casey, J. R., Cid, A., Lomas, M. W., Sohrin, Y., & Paytan, A. (2012). Phytoplankton responses to atmospheric metal deposition in the coastal and open-ocean Sargasso Sea. *Frontiers in Microbiology*, *3*(459), 1–15. https://doi.org/10.3389/fmicb.2012.00359

Mackey, K. R. M., van Dijken, G. L., Mazloom, S., Erhardt, A. M., Ryan, J., Arrigo, K. R., & Paytan, A. (2010). Influence of atmospheric nutrients on primary productivity in a coastal upwelling region. *Global Biogeochemical Cycles*, *24*, GB4027. https://doi.org/10.1029/2009GB003737

Maher, B. A., Prospero, J. M., Mackie, D., Gaiero, D., Hesse, P. P., & Balkanski, Y. (2010). Global connections between Aeolian dust, climate and ocean biogeochemistry at the present day and at the last glacial maximum. *Earth-Science Reviews*, *99*, 61–97. https://doi.org/10.1016/j.earscirev.2009.12.001

Marske, J. P., Pietruszka, A. J., Weis, D., Garcia, M. O., & Rhodes, J. M. (2007). Rapid passage of a small-scale mantle heterogeneity through the melting regions of Kilauea and Mauna Loa volcanoes. *Earth and Planetary Science Letters*, *259*, 34–50. https://doi.org/10.1016/j.epsl.2007.04.026

Martin, J. H. (1990). Glacial-interglacial CO_2 change: The iron hypothesis. *Paleoceanography*, *5*, 1–13. https://doi.org/10.1029/pa005i001p00001

McDermott, F., & Hawkesworth, C. (1991). Th, Pb, and Sr isotope variations in young island arc volcanics and oceanic sediments. *Earth and Planetary Science Letters*, *104*, 1–15. https://doi.org/10.1016/0012-821x(91)90232-7

McGee, D., Marcantonio, F., & Lynch-Stieglitz, J. (2007). Deglacial changes in dust flux in the eastern equatorial Pacific. *Earth and Planetary Science Letters*, *257*, 215–230. https://doi.org/10.1016/j.epsl.2007.02.033

Mix, A. C., Pisias, N. G., Rugh, W., Wilson, J., Morey, A., & Hagelberg, T. (1995). Benthic foraminiferal stable isotope record from Site 849, 0-5 Ma: Local and global climate changes. In N. G. Pisias, L. Mayer, T. Janecek, A. Palmer-Julson, & T. H. van Andel (Eds.), *Proceedings of the ODP,/Scientific results/138* (pp. 371–412). College Station, TX: Ocean Drilling Program.

Muhs, D. R., Budahn, J., Reheis, M., Beann, J., Skipp, G., & Fisher, E. (2007). Airborne dust transport to the eastern Pacific Ocean off southern California: Evidence from San Clemente Island. *Journal of Geophysical Research*, *112*, D13203. https://doi.org/10.1029/2006JD007577

Muhs, D. R., Budahn, J. R., Johnson, D. L., Reheis, M., Beann, J., Skipp, G., et al. (2008). Geochemical evidence for airborne dust additions to soils in Channel Islands National Park, California. *The Geological Society of America Bulletin*, *120*, 106–126. https://doi.org/10.1130/b26218.1

Murray, R. W., Knowlton, C., Leinen, M., Mix, A. C., & Polsky, C. H. (2000). Export production and carbonate dissolution in the central equatorial Pacific Ocean over the past 1 Myr. *Paleoceanography*, *15*(6), 570–592. https://doi.org/10.1029/1999PA000457

Park, S.-H., Lee, S.-M., Kamenov, G. D., Kwon, S.-T., & Lee, K.-Y. (2010). Tracing the origin of subduction components beneath the South East rift in the Manus Basin, Papua New Guinea. *Chemical Geology*, *269*, 339–349. https://doi.org/10.1016/j.chemgeo.2009.10.008

Parnell, A. (2020). Retrieved from https://github.com/andrewcparnell/simmr

Paytan, A., Mackey, K. R. M., Chen, Y., Lima, I. D., Doney, S. C., Mahowald, N., et al. (2009). Toxicity of atmospheric aerosols on marine phytoplankton. *Proceedings of the National Academy of Sciences of the United States of America*, *106*(12), 4601–4605.

Pettke, T., Halliday, A. N., Hall, C. M., & Rea, D. K. (2000). Dust production and deposition in Asia and the North Pacific Ocean over the Past 12 Myr. *Earth and Planetary Science Letters*, *178*(3–4), 397–413. https://doi.org/10.1016/S0012-821X(00)00083-2

Pichat, S., Abouchami, W., & Galer, S. J. G. (2014). Lead isotopes in the Eastern Equatorial Pacific record Quaternary migration of the South Westerlies. *Earth and Planetary Science Letters*, *388*, 293–305. https://doi.org/10.1016/j.epsl.2013.11.035

Rea, D. K. (1994). The Paleoclimatic record provided by eolian deposition in the deep sea: The geologic history of wind. *Reviews of Geophysics*, *32*, 159–195. https://doi.org/10.1029/93rg03257

Reimi, M. A., & Marcantonio, F. (2016). Constraints on the magnitude of the deglacial migration of the ITCZ in the Central Equatorial Pacific Ocean. *Earth and Planetary Science Letters*, *453*, 1–8. https://doi.org/10.1016/j.epsl.2016.07.058

Reimi, M. A., Marcantonio, F., Lynch-Stieglitz, J., Jacobel, A. W., McManus, J. F., & Winckler, G. (2019). The penultimate glacial termination and variability of the Pacific Intertropical Convergence Zone. *Geophysical Research Letters*, *46*, 4826–4835. https://doi.org/10.1029/2018GL081403

Ridame, C., & Guieu, C. (2002). Saharan input of phosphate to the oligotrophic water of the open western Mediterranean Sea. *Limnology & Oceanography*, *47*, 856–869. https://doi.org/10.4319/lo.2002.47.3.0856

Saukel, C., Lamy, F., Stuut, J.-B. W., Tiedemann, R., & Vogt, C. (2011). Distribution and provenance of wind-blown SE Pacific surface sediments. *Marine Geology*, *280*, 130–142. https://doi.org/10.1016/j.margeo.2010.12.006

Stancin, A., Gleason, J., Rea, D., Owen, R., Moorejr, T., Jr, Blum, J., & Hovan, S. (2006). Radiogenic isotopic mapping of late Cenozoic eolian and hemipelagic sediment distribution in the east-central Pacific. *Earth and Planetary Science Letters*, *248*, 840–850. https://doi.org/10.1016/j.epsl.2006.06.038

Stancin, A. M., Gleason, J. D., Hovan, S. A., Rea, D. K., Owen, R. M., Moore, T. C., Hall, C. M., et al. (2008). Miocene to recent eolian dust record from the Southwest Pacific Ocean at 40 degrees S latitude. *Palaeogeography Palaeoclimatology Palaeoecology*, *261*, 218–233.

Trudgill, M. D., Shuttleworth, R., Bostock, H. C., Burke, A., Cooper, M. J., Greenop, R., & Foster, G. L. (2020). The flux and provenance of dust delivered to the SW Pacific during the Last Glacial Maximum. *Paleoceanography and Paleoclimatology*, *35*, e2020PA003869. https://doi.org/10.1029/2020PA003869

Vallelonga, P., Gabrielli, P., Balliana, E., Wegner, A., Delmonte, B., Turetta, C., et al. (2010). Lead isotopic compositions in the EPICA Dome C ice core and southern hemisphere potential source areas. *Quaternary Science Reviews*, *29*, 247–255. https://doi.org/10.1016/j.quascirev.2009.06.019

White, W. M., Albarède, F., & Télouk, P. (2000). High-precision analysis of Pb isotope ratios by multi-collector ICP-MS. *Chemical Geology*, *167*, 257–270. https://doi.org/10.1016/s0009-2541(99)00182-5

Winckler, G., Anderson, R. F., Fleisher, M. Q., McGee, D., & Mahowald, N. (2008). Covariant glacial-interglacial dust fluxes in the equatorial Pacific and Antarctica. *Science*, *320*, 93–96. https://doi.org/10.1126/science.1150595

Worthy, T. H., & Grant-Mackie, J. A. (2003). Late-Pleistocene avifaunas from Cape Wanbrow, Otago, South Island, New Zealand. *Journal of the Royal Society of New Zealand*, *33*(1), 427–485. https://doi.org/10.1080/03014223.2003.9517738

Wu, J., Rember, R., Jin, M., Boyle, E. A., & Flegal, A. R. (2010). Isotopic evidence for the source of lead in the North Pacific abyssal water. *Geochimica et Cosmochimica Acta*, *74*, 4629–4638. https://doi.org/10.1016/j.gca.2010.05.017

Xie, R. C., & Marcantonio, F. (2012). Deglacial dust provenance changes in the Eastern Equatorial Pacific and implications for ITCZ movement. *Earth and Planetary Science Letters*, *317–318*, 386–395. https://doi.org/10.1016/j.epsl.2011.11.014

Yang, S. L., & Ding, Z. L. (2003). Color reflectance of Chinese loess and its implications for climate gradient changes during the last two glacial-interglacial cycles. *Geophysical Research Letters*, *30*(20), 2058. https://doi.org/10.1029/2003GL018346

Yokoo, Y., Nakano, T., Nishikawa, M., & Quan, H. (2004). Mineralogical variation of Sr-Nd isotopic and elemental compositions in loess and desert sand from the central Loess Plateau in China as a provenance tracer of wet and dry deposition in the northwestern Pacific. *Chemical Geology*, *204*(1), 45–62. https://doi.org/10.1016/j.chemgeo.2003.11.004

Ziegler, C. L., Murray, R. W., Plank, T., & Hemming, S. R. (2008). Sources of Fe to the equatorial Pacific Ocean from the Holocene to Miocene. *Earth and Planetary Science Letters*, *270*, 258–270. https://doi.org/10.1016/j.epsl.2008.03.044

Zubrick, C. M., Gallon, C., & Flegal, A. R., (2017). Historic and industrial lead within the Northwest Pacific Ocean evidenced by lead isotopes in Seawater. *Environmental Science & Technology*, *51*, 1203–1212. https://doi.org/10.1021/acs.est.6b04666